DEVELOPMENT OF AN ISOLATED BI-DIRECTIONAL DC-DC CONVERTER FOR OFF-GRID PV/WIND HYBRID AND ON-GRID PV SYSTEM

Clark Darwin M. Gozon
Electrical Engineering Dept., University of Science and Technology of Southern Philippines,
Cagayan de Oro City 9000, Philippines
clarkdarwin.gozon@ustp.edu.ph

ABSTRACT: *The objective of this study is to enhance the effectiveness of renewable energy facilities at the University of Science and Technology of Southern Philippines (USTP). This was achieved by combining the 5kW, 46Vdc on-grid solar photovoltaic system with the 5kW, 96Vdc off-grid solar photovoltaic/wind hybrid system. A bi-directional DC-DC converter was developed to transfer the excess power from 48V RE system to 96V RE system and vice-versa. To validate the approach, simulations were conducted using Matlab-Simulink, and practical tests were performed in both laboratory and real-world conditions. The resulting prototype demonstrated remarkable efficiency, exceeding 90% in power transfer for both boosting and reducing modes. The outcomes further confirmed the feasibility of the energy exchange concept between the renewable energy plants through the developed converter.*

Keywords- RE Integration, Bi-directional Converter, Push-pull DC-DC converters, Hybrid RE systems.

I. INTRODUCTION

In the past years, due to the electricity supply deficit in Mindanao, Philippines, 3 to 7 hours of rotating power interruption was implemented. Thus, electricity consumers were finding alternative sources of electrical energy. Options include solar photovoltaic (PV) and wind turbines. Among the reasons are that they can be quickly installed in backyards and rooftops, are renewable, with minimal maintenance, are modular, and are configurable in different ways (i.e. off-grid or on-grid, with or battery, etc.). Although as of now electricity costs from solar PV and wind systems are higher compared to that of utility, parity with these systems is far ahead. This is due to the decreasing trend of PV and wind energy system prices and increasing price of utility rates. This can make investing in such hybrid systems beneficial. Surplus energy from the plant could be exported to the utility grid at a near utility rate (today's setting) or equal to the utility rate (future). Also, if utility time of use (TOU) pricing is applicable, this makes it possible for small-scale power plant owners to deliver PV power at peak hours when the electricity rate is high and consume utility power at off-peak hours while charging the battery(if with battery) from the sun and/or utility. Moreover, battery costs can be avoided since it is not necessary for a grid-connected PV/wind turbine system.

As mentioned, one key feature of solar PV (photovoltaic)/wind turbine is it's being modular. Modular means its capacity can be increased as needed. The capacity of a solar PV plant is determined by the number of modules connected in series and/or in parallel. The capacity of wind turbines could be increased by adding more wind turbines. Furthermore, the capacity of an existing system could be increased either by adding PV modules/turbines or by integrating two existing systems to deliver bulk power. In addition, integrating two or more RE systems may increase the overall system efficiency. A problem however arises when integrating two or more PV systems with different DC (direct current) bus voltages since the same voltage amplitude is a requirement for them to be connected in parallel.

Such a special case of hybrid systems with different DC bus voltages is encountered in USTP, Mindanao, Philippines. They wanted to integrate two of their systems to improve system efficiency. The integration of these two systems was the main concern of this study.

1.1. RE plants in USTP

Previously the Hybrid RE systems installed in MUST composed a 15kW off-grid PV/wind hybrid, a 5kW off-grid PV/wind hybrid, and a 5kW on-grid PV, totaling 25 kW. They wanted to integrate the two 5 kW systems. The following

sections discuss these two RE systems with their block diagrams.

Table 1 is the summary of the specification of two 5 kW solar PV systems installed in MUST.

Table 1. Solar PV installed in MUST

	RE System 1	RE System 2
Size	5kW	5kW
Wind installed capacity	0 W	300 W
PV installed capacity	5kW	4.8kW
Configuration	Grid Connect	Grid Interactive
DC voltage	48V	96V
Battery	Yes	Yes
No. of battery	8	8
Rated Watts per panel	250W	200W
Cell technology	Polycrystalline	Polycrystalline
No. of Panels	20	24

II. RE SYSTEM INTEGRATION SCHEME

To integrate the RE systems, an isolated bi-directional DC-DC converter was used. DC-DC converter was connected between the battery busses of the RE systems as shown in Figure 1. The converter operated in two modes; Step-up mode and Step-down mode with individual sets of conditions.

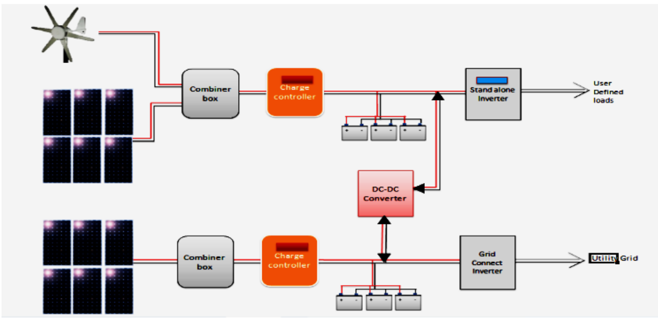

Figure 1. Block diagram with proposed DC-DC converter

In step-up mode, when the utility grid is not available, the on-grid battery voltage is fully charged or above the threshold voltage (above 50V), and stand alone battery voltage is lesser than the full charge voltage, DC-DC converter operates as step-up (boost) converter since grid-connected RE system has lower DC bus voltage compared to stand alone RE system. The power will flow from the grid-connected RE battery bus through the proposed isolated DC-DC- converter to the stand-alone RE system. Energy can be directly supplied to the defined user's loads through a stand-alone inverter and/or can be charged to the stand-alone RE batteries with a condition depending on the state of the batteries and the demand of the user load.

Step-down mode: when the utility grid is available, the on-grid battery voltage is lesser than the full charge voltage, and the stand-alone battery is fully charged or above the threshold voltage (above 100V). DC-DC converter operates as a step-down (buck) converter. The power will flow from a stand-alone RE system to a grid-connected RE system. Energy can be directly delivered to the utility grid and store the excess power in grid batteries.

III. BI-DIRECTIONAL DC-DC CONVERTER DESIGN

The isolated bidirectional DC-DC converter is mainly composed of the following components: a Microcontroller unit, high-frequency transformer, voltage, and current sensors, MOSFET drivers, LCD, filters and transient suppressor, and power supply unit.

3.1 Proposed topology

Several types of DC-DC converters exist, and each of these types of converters is suitable for specific types of applications. In the integration of the two RE plants, the following are the minimum criteria for choosing the topology employed in this paper:

a. Provide electrical isolations between the two RE systems
b. Provide a bi-directional flow of power

Common isolated DC-DC converters were compared in terms of their power, transformer design, efficiency, cost, and number of components. A push-pull topology was chosen since it has the least number of semiconductors, making it cost-effective. Also because the push-pull scheme has a transformer, it can provide electrical isolation between two inputs which adds safety and protection to the RE systems. Moreover, with some modifications, push-pull topology can provide the bidirectional flow of power for the integration of the system under study. Figure 2 shows the basic push-pull design.

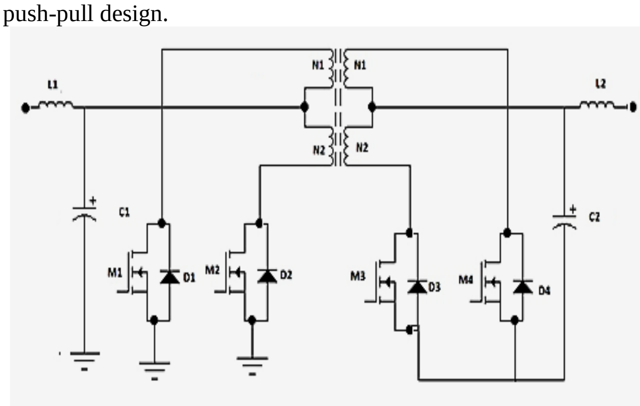

Figure 2. Modified Push-pull bi-directional DC-DC converter topology

This circuit was obtained by modifying the uni-directional push-pull converter by adding two power transistors and power diodes on the secondary side of the transformer. Components are arranged like a mirror of the primary side of the converter. The coils N1 and N2 of the transformer have the same number of turns and are lesser number of turns than N3 and N4. The converter will operate in two modes: step-up and step-down mode.

In a steady state of operation, for step-up mode, M_1 is ON for the period of T_{ON}, and the dot end of the windings becomes positive concerning the non-dot end. The diode D_1 and D_2 become reverse-biased and the diode D_4 becomes forward-biased. Thus, the diode D_4 provides the path to the output inductor current I_L through the transformer secondary N_{S1}. As the input voltage, V_{IN} is applied to the transformer primary winding N_{P1}, a reflected primary voltage appears in the transformer secondary.

At the end of the T_{ON} period, the switch M_1 is turned OFF and remains off for the rest of the switching period TS. The switch M_2 will be turned ON after half of the switching period TS/2, Thus, during the T_{OFF} period, both of the switches (M_1 and M_2) are OFF. When switch M_1 is turned OFF, the body diode of the switch provides the path for the leakage energy stored in the transformer primary, and the output rectifier diode D_3 becomes forward-biased. As the diode D_3 becomes forward-biased, it carries half of the inductor current through the transformer secondary N_{S2} and half of the inductor current is carried by the diode D_2 through the transformer secondary N_{S2}. This results in equal and opposite voltages applied to the transformer secondary, assuming both secondary windings N_{S1} and N_{S2} have an equal number of turns.

3.2 High-frequency transformer

Transformer for switch mode dc-dc converters is a special type of transformer because it operates at high-frequency voltage/current. To calculate the number of turns of the coil transformer, an arbitrary choice should be made on which side of the transformer to calculate the number of turns first. The number of turns was calculated by:

$$N = \frac{10^8 V_m D}{\Delta\beta_{\max} f A_e} \quad (1)$$

or

$$N = \frac{10^8 V_m D}{2\beta_{\max} f A_e} \quad (2)$$

Where: V_m is the peak input voltage, V is the operating PWM duty cycle, β_m is the maximum magnetic flux of the core in Gauss, and A_e is the cross-sectional area of the core in cm^2.

To find the number of secondary turns to support the secondary voltage, the turns ratio a has to be calculated and is given by;

$$a = \frac{V_H}{V_L} = \frac{N_H}{N_L} \quad (3)$$

Where: V_H is is the voltage at the high voltage side, V_L is the voltage at the low voltage side N_H is the number of turns at the high voltage side, and V_L is the number of turns at the low voltage side.

To check if the coils will fit in the selected core, the minimum window area A_w of the core was calculated by

$$A_w = \frac{2W_{A1}N_H + 2W_{A2}N_L}{k} \quad (4)$$

Wheresub-A1is the minimum area occupied by coil for high voltage sidsusususususub-A2 W_{A2} is the minimum area occupied by coil for low voltage side, and k is the fill factor since the coils were not perfectly wound. The value of k is always lesser than 1. W_{An} can be calculated by

$$W_{A1orA2} = I_H orL / J \quad (5)$$

Where: I_H is the maximum allowable current to flow in the conductor and J is current density A/m2. The good value of J for copper is 4.5A/mm2.

The last thing to consider in the design of a high-frequency transformer is the conductor. Selecting a conductor for a high-frequency transformer is crucial because of the skin effect; where the current flowing in the conductor is not flowing through the area of the conductor. This means, choosing a large conductor for a high-frequency transformer is not beneficial. Hence, a bundle of smaller sizes of conductor or conductor tape is the best choice. The minimum cross-sectional diameter of wires to be bundled can be calculated by;

$$d = \frac{144}{\sqrt{f}} \quad (6)$$

Table 2 shows the list of important parameters needed to design a high-frequency transformer.

Table 2. Parameters of the proposed high-frequency transformer.

Parameter	Value
Low side voltage (V_L)	48 V nominal
High side voltage (V_H)	96 V nominal
Low side voltage (I_L)	100 A max
High side voltage (I_H)	50 A max
Switching frequency (f)	31.37 kHz
Rated power	5 kW

From equations 1 to 6 and the required design parameters of the high-frequency transformer, the number of turns, core size, and conductors can be determined. Table 3 is a summary of the specifications of the transformer.

Table 3. Summary of results for high-frequency transformer

High side # of turns	6 turns per coil
Low side # of turns	3 turns per coil
High side conductor	30 strands of gauge #23 magnetic wire
Low side conductor	60 strands of gauge #23 magnetic wire
Transformer core	UI ferrite core, cross-sectional area of 6.83 cm2 from EPCOS

3.4 Filter designs

3.4.1 Inductor

In designing the filter inductor the key parameter needed was the peak-to-peak current that the inductor should not permit for some time. The inductance of inductor L (in Henry) is given by the equation below.

$$L = \frac{V_{in}\Delta t}{\Delta i} \qquad (7)$$

Where: V_{in} is the input voltage, Δt is the differential time for current to change, and Δi is the allowed change of current.
The number of turns can be calculated from:

$$L = 0.004\mu h N^2 \frac{D_1 - D_2}{D_1 + D_2} \qquad (8)$$

Where: μ is the relative permeability of the core, h is the thickness of the core, D_1 is the outer diameter of the core, D_2 is the inner diameter of the core, and N is the number of turns. For the formula, D_1/D_2 should be lesser than 1.75 else, the formula below should be used;

$$L = 0.0002\mu h N^2 \ln\frac{D_1}{D_2} \qquad (9)$$

Assumptions and design requirements for the design of the choke inductor are summarized in Table 4.

Table 4. Design requirements for the inductor.

Parameter	High Voltage Side	Low Voltage Side
Vin	96V	48V
Δi	50A	25A
Δt	1 mSec	
μ	4200 r N30 Core Material)	

From the formula presented, the on-grid side (low voltage side) winding was 3 turns for each winding, and the off-grid side (high voltage side) winding was 6 turns for each winding. Conductors for the coils for the on-grid side were made from 2 by 30 stands of gauge #23 magnetic wires and coils for the off-grid side were 30 stands of gauge #23 magnetic wires. The core used was a UI ferrite core with a cross-sectional area of 6.83cm^2 from EPCOS.

3.4.2 Filter Capacitor

The main function of the capacitor was to maintain the constant output voltage. It made the output voltage ripple almost free.

$$C = \frac{I_{in}\Delta t}{\Delta v} \qquad (10)$$

or

$$C = \frac{I_{in}}{f\Delta v} \qquad (11)$$

Where: I_{in} current, Δt is the differential time for current to change, f is the PWM frequency, and Δv is the allowed change of voltage. The design requirement for selecting the filter capacitor is shown in the table.

Table 5. Design requirements for the capacitor.

Parameter	High Voltage Side	Low Voltage Side
I_N	50 A	25 A
Δv	2 V	1 V
F	31.37 kHz	

IV. SIMULATION MODELS AND RESULTS

Before the fabrication, an initial validation through computer simulation was done in Matlab-Simulink to support the concept of using back-to-back push-pull configuration to provide isolated bidirectional power flow of a DC-dc converter.

4.1 Simulation models

The control circuit was designed based on the desired switching frequency and the duty cycle. The switching frequency used was 33.317 kHz. Hence a 16MHz microcontroller easily generated this frequency. The design duty cycle varied from 60%-90%. Figure 3 shows the Matlab-Simulink model used to generate the complementary MOSFET gate signals.

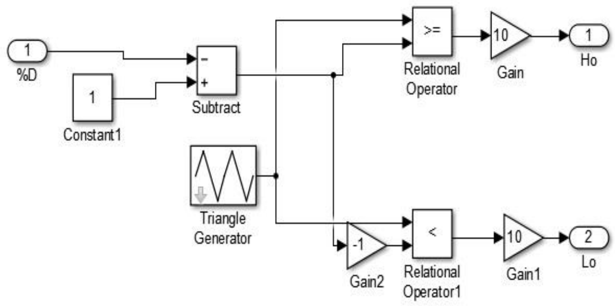

Figure 3. Simulation mode for MOSFET gate signal control

Figure 4 is the simulation model of the push-pull converter. The model consists of four MOSFETs connected with a PWM controller. Each terminal end of each side is connected to a DC power source.
The circuit shown in Figure 4 was reconfigured to operate as a buck converter or boost converter. To determine the individual performance of the said configurations, it was simulated in separate independent models: Step-up mode and Step-down mode.

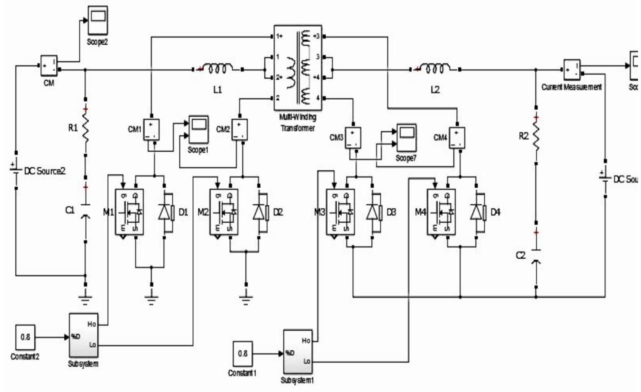

Figure 4. Simulation model of the designed isolated bi-directional DC-DC converter

4.2 Boost (step-up) mode

To simulate the step-up mode operation, it was tested by removing the input source for the step-down mode and was replaced by a resistive load connected to a voltage with a scope to determine the desired output.

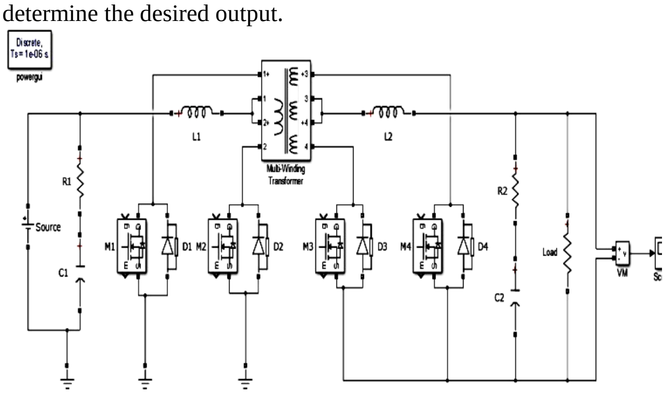

Figure 5. Matlab-Simulink model for boost mode

Figure 6 is the simulated voltage response of the isolated dc-dc converter in step-up mode. The blue line is the low side input voltage and the red line is the output voltage at the high side.

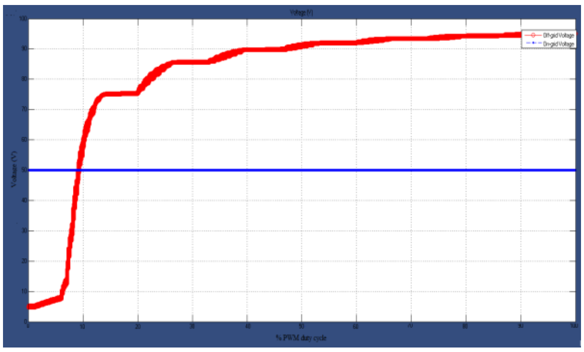

Figure 6. Simulated Step-up mode voltage response with respect to PWM duty at 50V input.

4.3 Buck (step-down) mode

The same operation was done in step-up mode. The right side of the converter was tested by removing the input source for the step-up mode and replacing it with a resistive load connected to a voltage measurement with scope to determine the desired output. Figure 7 shows the Matlab-Simulink Model and Figure 8 shows the simulation result. The red line is the input voltage at the high side of the converter and the blue line is the output at the other side.

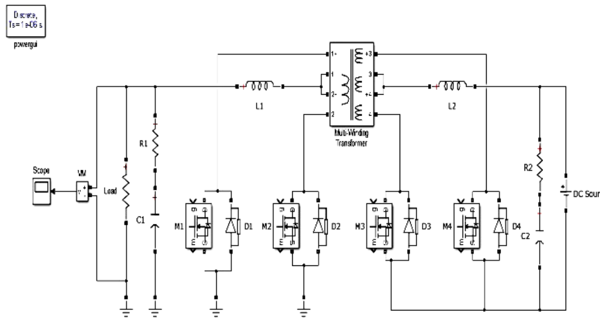

Figure 7. Matlab-Simulink model for buck mode

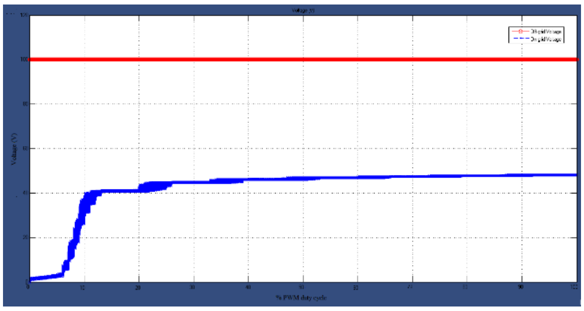

Figure 8. Simulated Step-down mode voltage response with respect to PWM duty at 100V input.

V. DEVELOPED ISOLATED BI-DIRECTIONAL DC-DC CONVERTER

Figure 9 is a photograph of the developed isolated bi-directional DC-DC converter showing the major components.

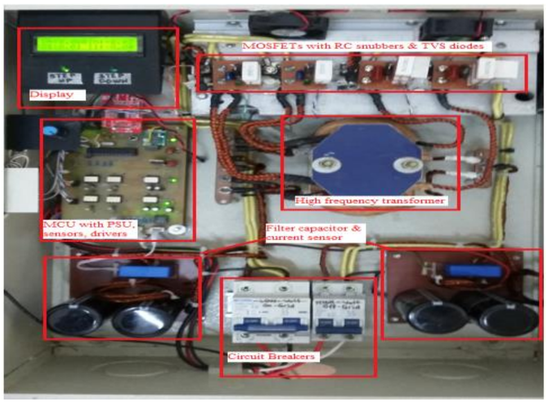

Figure 9. Photograph of the developed isolated bi-directional DC-DC converter.

5.1 Voltage Vs PWM duty response

To test the voltage response of the developed isolated bi-directional DC-DC converter concerning the PWM duty cycle, a custom program of MCU was created for both modes. The MCU program increments the pulse width modulation's duty cycle until it reaches 100%. In every increment of the PWM duty cycle, THE MCU will output an equivalent response to input and output voltage. Figure 10 and Figure 11 are voltages of the isolated bi-directional DC-DC converter in response to the change of the PWM duty cycle. It can be observed that the responses of the output voltages are not linear about the change of PWM duty due to this is because the core was designed to operate at near saturation. Moreover, the experimental results coincide with the simulation results.

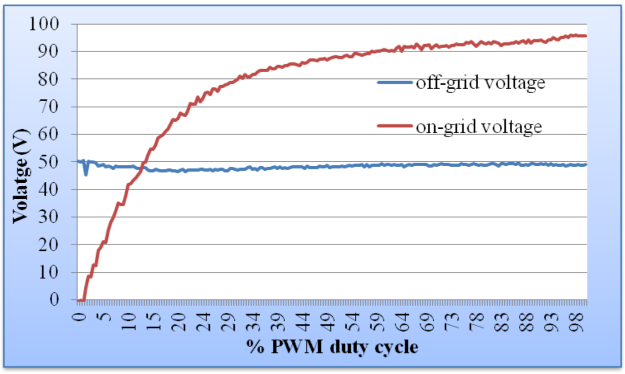

Figure 10. Step-up mode voltage response with respect to PWM duty 50V input.

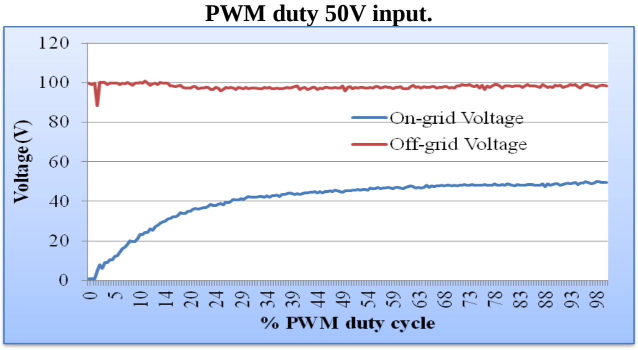

Figure 11. Step-down mode voltage response with respect to PWM duty at 100V input.

5.3 DC-DC converter system bench efficiency test

One of the measuring performance indicators of any machine or device is efficiency. The developed isolated bi-directional DC-DC converter was subjected to a bench efficiency test. Efficiency for both step-up and step-down modes was determined Equation for determining the efficiency is shown below

$$\eta = \frac{Power_{output}}{Power_{output}} x100\% \qquad (12)$$

Figures 12 and 13 are the scatter plots of the efficiency for both modes. It can be observed in the efficiency test result that the converter performs well at higher power output and performs less at lower power. The maximum efficiency achieved during the test can be reached to as much as 90% at around 400 - 600 watts.

Efficiency can still increase if the output power is increased further since the trends of efficiencies are still increasing. Hence, the test done in determining the efficiencies of the isolated bidirectional DC-DC convert for both boost (step-up) and buck (step-down) was not done at its maximum limit due to resource limitations such as input power limit, dump load capacity limit, and measuring instrument limitations.

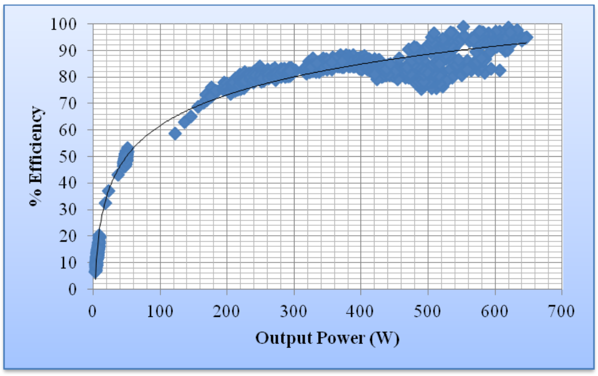

Figure 12. Scatter plot of efficiency test for buck mode.

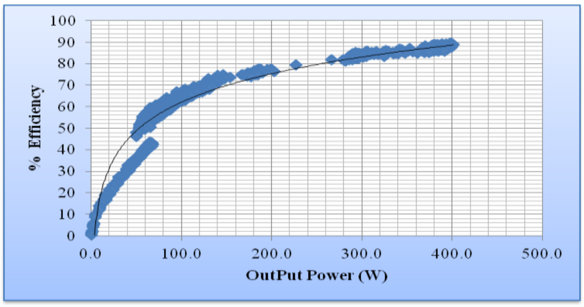

Figure 13. Scatter plot of efficiency test for boost mode.

5.4 Actual RE systems integration using the developed converter

After thorough calibration and bench testing, the developed isolated bi-directional DC-DC converter was tested on the actual RE systems. Figure 14 shows the isolated bi-directional DC-DC converter connected to the 5kW on-grid and off-grid 5kW systems. The measuring instruments and monitoring software are provided to measure the system's performance. The prototype was connected to the battery terminals of the two RE systems as shown in figure 9.

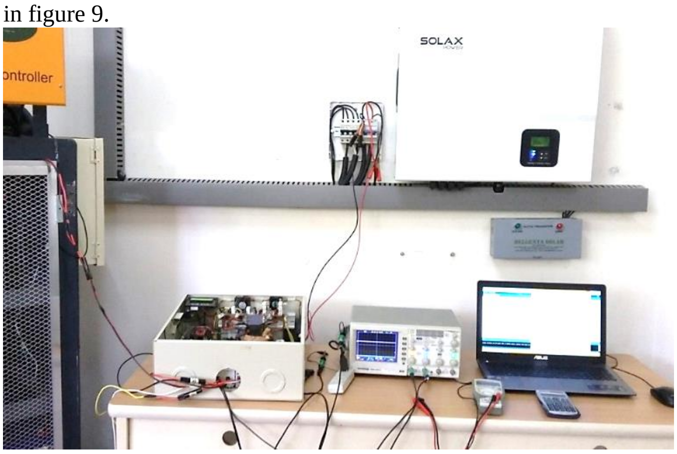

Figure 14. Bi-directional DC-DC converter temporarily connected to 5kW on-grid and 5kW off-grid systems.

During the test, the grid was on, the converter operates in buck mode. The power flows from an off-grid system to an on-grid system. Negative power means the RE system delivers power. Positive power means RE system absorbers power. To test the MCU algorithm employed in this study, a power grid outage was simulated by turning off the grid circuit breaker. Figure 15 shows the power flow response of the isolated bi-directional DC-DC converter. As observed in the figure, when the grid is out, the converter operates now in boost mode. The direction of the flow of power was reversed.

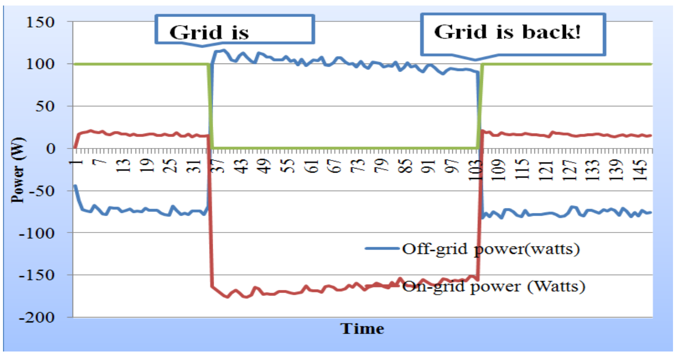

Figure 15. Voltage fluctuations during mode transitions.

VI. CONCLUSIONS

From simulations, experimentation, and actual tests done in the developed converter, it can be concluded that the idea of integrating the two RE systems using an isolated bi-directional DC-DC converter can solve the problem of integrating two RE systems with different DC/battery bus voltages. Simulated and experimental voltage response for both step-up and step-down modes shows significant coherence. The developed prototype also shows an impressive efficiency of more than 90% for both modes.

VII. REFERENCES

[1] Cultura, A. B., and Ziyad, S.M., "Design and Analysis of a 24 Vdc to 48Vdc Bidirectional DC-DC Converter Specifically for a Distributed Energy Application"," *Energy and Power Engineering,* vol. no.4, pp. 315-323, (2012)

[2] Lee, S.W., and et.al, "New High Efficient Bi-directional DC/DC Converter in the Dual Voltage System," *Journal of Electrical Engineering & Technology,* vol. 1, no. 3, pp. 343-350, (2006)

[3] Citko, S. and Jalbrzykowski, T., "A bidirectional DC_DC Converter for Renewable Energy Systems," *Bulletin of the Polish Academy of Sciences, Technical Sciences,* vol. 57, no. 4, (2009)

[4] Aparnathi, R. and Dwivedi, V.V., "Maximum Power Point Tracking in PV System with Industry Applications," *International Journal of Power Electronics and Drive System (IJPEDS),* vol. 3, no. 4, pp. 417-423, (2013)

[5] Akagi, S.I. and et.al, "Bidirectional DC/DC Converter for an Energy Storage System," *IEEE,* vol. 1, no. 1, pp. 4244-0714, (2007)

[6] Ramu, G., "Analysis and Design of an Isolated Bidirectional DC-DC Converter for Hybrid Systems," *Middle East Journal of Scientific Research,* vol. 19, no. 7, pp. 960-965, (2014)

[7] Kumar, S. and Sydulu, M., "Bidirectional DC-DC Converter for Integration of Battery Energy Storage System with DC Grid," *Proceedings of IRF International Conference,* Vols. ISBN: 978-93-82702-58-0, pp. 1-5,(2014)